Exploring the Violation of Lorentz Invariance using Atmospheric Neutrinos at INO-ICAL

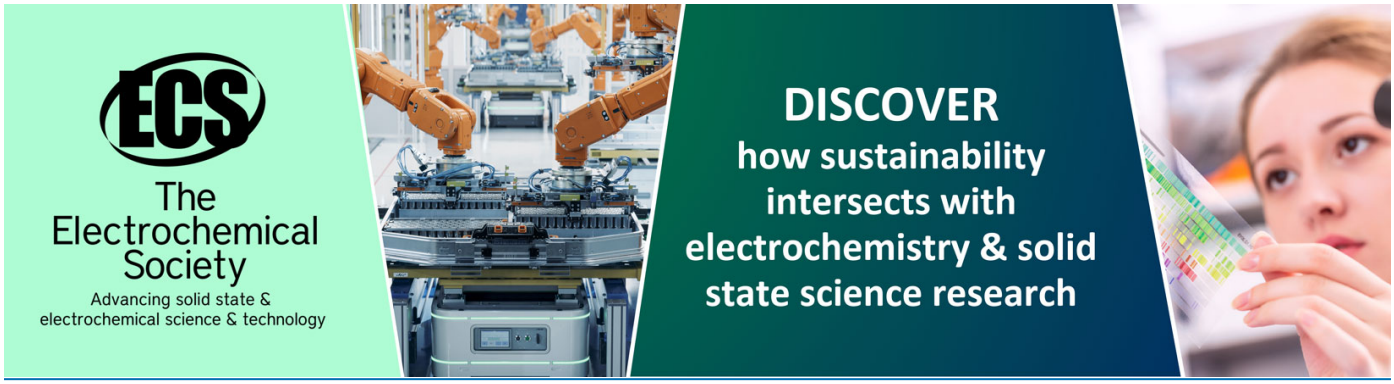

Journal of Physics: Conference Series **2156** (2022) 012238 doi:10.1088/1742-6596/2156/1/012238

Exploring the Violation of Lorentz Invariance using Atmospheric Neutrinos at INO-ICAL

Sadashiv Sahoo[1,2], **Anil Kumar**[1,2,3], **Sanjib Kumar Agarwalla**[1,2,4]

[1]Institute of Physics, Sachivalaya Marg, Sainik School Post, Bhubaneswar 751005, India
[2]Homi Bhabha National Institute, Anushakti Nagar, Mumbai 400094, India
[3]Applied Nuclear Physics Division, Saha Institute of Nuclear Physics, Block AF, Sector 1, Bidhannagar, Kolkata 700064, India
[4]International Centre for Theoretical Physics, Strada Costiera 11, 34151 Trieste, Italy

E-mail: sadashiv.sahoo@iopb.res.in

Abstract. We explore the signature of Lorentz Invariance Violation (LIV) in the Standard Model Extension framework by observing the atmospheric neutrinos and antineutrinos separately with the help of magnetized Iron Calorimeter (ICAL) detector at the proposed India-based Neutrino Observatory (INO). Using 500 kt·yr exposure of ICAL, we place stringent bounds on the CPT-violating LIV parameters $a_{\mu\tau}, a_{e\mu}$, and $a_{e\tau}$ (one-at-a-time) at 95% C.L. (1 d.o.f). We demonstrate the advantages of charge identification capability and hadron energy information at ICAL while constraining these LIV parameters. We also explore interesting correlations among various LIV parameters.

1. Introduction

The Lorentz Symmetry has been assumed in Quantum Field Theory (QFT) and General Theory of Relativity (GTR) whereas at Planck scale physics ($\sim$ M_P), the attempts to unify gravity with the Standard Model (SM) gauge fields allow the Lorentz Symmetry Breaking (LSB). In the Effective Field Theory (EFT), the effects of LSB on the low energy observables are suppressed by an order of $1/M_P$. In this paper, we study the CPT-violating Lorentz Invariance Violation (LIV) parameters induced due to the spontaneous LSB, which is prescribed in a proposed model of the string theory in Ref [1]. The CPT-violating LIV parameters have more significant effects on the neutrino propagations. So, an atmospheric neutrino detector like magnetised Iron Calorimeter (ICAL) at the India-based Neutrino Observatory (INO) [2], which has an excellent muon energy resolution of about 10 to 15% in the reconstructed muon energy range of 1 to 25 GeV and zenith angle resolutions of less than 1° over 15 to 12800 km range of baselines with the Charge Identification (CID) capability, can provide a unique window to explore CPT-violating LIV parameters for neutrino and antineutrino events separately. In principle, both time and spatial components of CPT-violating LIV parameters can be explored using atmospheric neutrinos. However, due to the limited statistics of the prospective data with an exposure of 500 kt·yr at ICAL, we consider only the time component of the CPT-violating LIV parameters $(a_{\mu\tau}, a_{e\mu}, a_{e\tau})$ in the Sun-centered celestial equatorial frame mentioned in Ref [3].

2. Formalism

We consider the effective Hamiltonian ($\mathcal{H}_{\text{eff}}$) in the three-flavor basis, which includes the interactions due to the time components of the CPT-violating LIV parameters along with the interactions of the left-handed neutrinos propagating through the Earth's matter,

$$\mathcal{H}_{\text{eff}} = \frac{1}{2E} U \begin{pmatrix} 0 & 0 & 0 \\ 0 & \Delta m^2_{21} & 0 \\ 0 & 0 & \Delta m^2_{31} \end{pmatrix} U^\dagger \pm \begin{pmatrix} a_{ee} & a_{e\mu} & a_{e\tau} \\ a^*_{e\mu} & a_{\mu\mu} & a_{\mu\tau} \\ a^*_{e\tau} & a^*_{\mu\tau} & a_{\tau\tau} \end{pmatrix} \pm \sqrt{2} G_F N_e \begin{pmatrix} 1 & 0 & 0 \\ 0 & 0 & 0 \\ 0 & 0 & 0 \end{pmatrix}. \quad (1)$$

Here, the first term is the standard kinematics, where E is the neutrino energy, U is the standard 3×3 PMNS matrix, Δm^2_{31} and Δm^2_{21} are the atmospheric and the solar mass-squared splittings, respectively. The second term contains the CPT-violating LIV parameters $a_{\alpha\beta}$, where α, β are the flavor indices. The last term contains the standard matter interaction potential ($\sqrt{2}G_F N_e$) arising due to the neutrino-electron forward elastic scattering, where G_F is Fermi weak coupling constant, and N_e is the electron number density inside the Earth's matter. The $\pm$ sign in the last two matrices are used to represent the $\mathcal{H}_{\text{eff}}$ with (+) sign for the case of left-handed neutrino and (-) sign for right-handed antineutrino. Note, these sign-changing scenarios for $a_{\alpha\beta}$ are due to the inbuilt structure of spontaneous LIV (see Appendix A of Ref [4]), whereas for the matter-potential, is due to change of neutrino helicity. Since, more than 98% of the events at ICAL are contributed via disappearance channel $P(\nu_\mu \to \nu_\mu)$ where $a_{\mu\tau}$ is expected to have dominant effect, we plot the muon survival oscillograms with non-zero $a_{\mu\tau}$ keeping null values

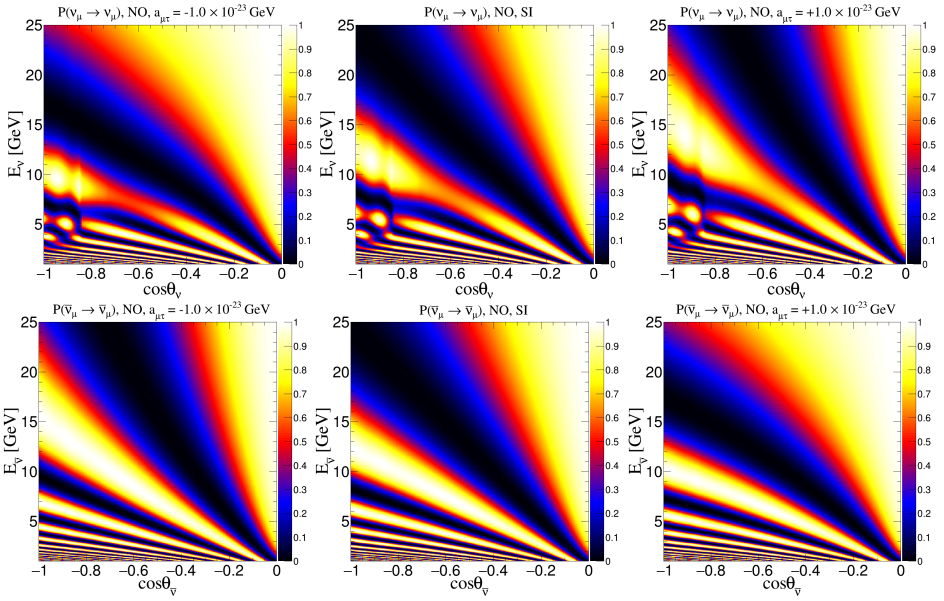

Figure 1. The survival oscillograms of ν_μ(top panels) and $\bar{\nu}_\mu$(bottom panels) are plotted in (E_ν, $\cos\theta_\nu$) plane including Earth's matter effect using PREM profile. Oscillation parameters used-in are given in Table 1. The values of $a_{\mu\tau}$ are considered as -1.0×10^{-23} GeV, 0, and 1.0×10^{-23} GeV in the left, middle and right columns, respectively. These figures have been taken from Ref. [4].

$\sin^2 2\theta_{12}$	$\sin^2 \theta_{23}$	$\sin^2 2\theta_{13}$	Δm^2_{eff} (eV^2)	Δm^2_{21} (eV^2)	δ_{CP}	Mass Ordering
0.855	0.5	0.0875	2.49×10^{-3}	7.4×10^{-5}	0	Normal (NO)

Table 1. Oscillation parameters used in this analysis are taken from Table 1 of Ref. [4]. Here, Δm^2_{eff} is related to Δm^2_{31} as expressed in [5].

of $a_{e\mu}$ and $a_{e\tau}$ in Fig. 1. Here, we use the oscillation parameters as given in Table. 1 which are consistent with the present global fits values [6]. In Fig. 1, the middle column shows the survival oscillograms of $\nu_\mu(\bar{\nu}_\mu)$ with Earth's matter effect for $a_{\mu\tau} = 0$ whereas the exterme columns show with the non-zero values of $a_{\mu\tau}$. For a given non-zero value of $a_{\mu\tau}$, the bendings of oscillation vallies in the ν_μ (top panels) and $\bar{\nu}_\mu$ (bottom panel) survival oscillograms are almost mirror images to each other.

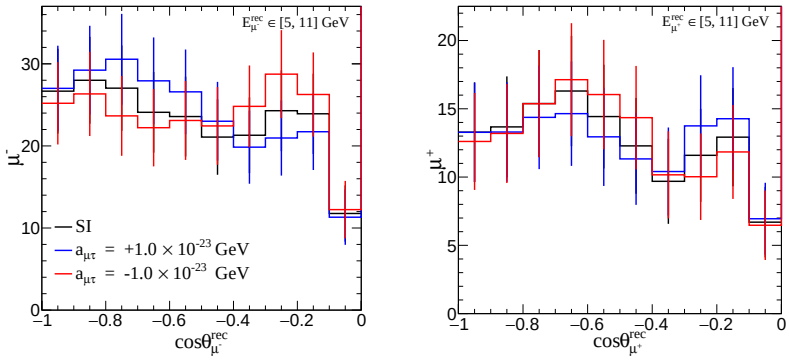

Figure 2. The distributions of reconstructed μ^- (left panel) and μ^+ (right panel) events (Y-axis) over reconstructed zenith angles (X-axis) within the reconstructed energy range of 5 – 11 GeV at the ICAL detector for an exposure of 500 kt·yr. These figures have been taken from Ref. [4].

We explore the non-zero values of CPT-violating LIV parameters $(a_{\mu\tau}, a_{e\mu}, a_{e\tau})$ considering one-at-a-time in a full three-flavor neutrino paradigm, using the oscillation parameters as given in Table. 1, which calculated numerically with Earth's PREM profile. The method of generating prospective data has been discussed in Section 5 of Ref [4]. Figure 2 shows the impacts of $a_{\mu\tau}$ on the reconstructed μ^- and μ^+ events for an exposure of the 500 kt·yr within the range of 5 – 11 GeV of reconstructed muon energy. Here, the black curves correspond to the events for $a_{\mu\tau} = 0$, whereas the blue and red curves correspond to the events for $a_{\mu\tau} = +1.0 \times 10^{-23}$ GeV and $a_{\mu\tau} = -1.0 \times 10^{-23}$, respectively. The error bars represent the statistical uncertainties.

3. Results

In Fig. 3, we compare the $\Delta\chi^2$ sensitivity to constrain the $a_{\mu\tau}, a_{e\mu}, a_{e\tau}$ one-at-a-time with 95% C.L with CID and without CID. We marginalize $\Delta\chi^2$ over oscillation parameters $\sin^2\theta_{23}$ ranging $[0.36, 0.66]$, Δm^2_{eff} ranging $[2.1, 2.6] \times 10^{-3}$ eV^2, and both normal and inverted mass orderings.

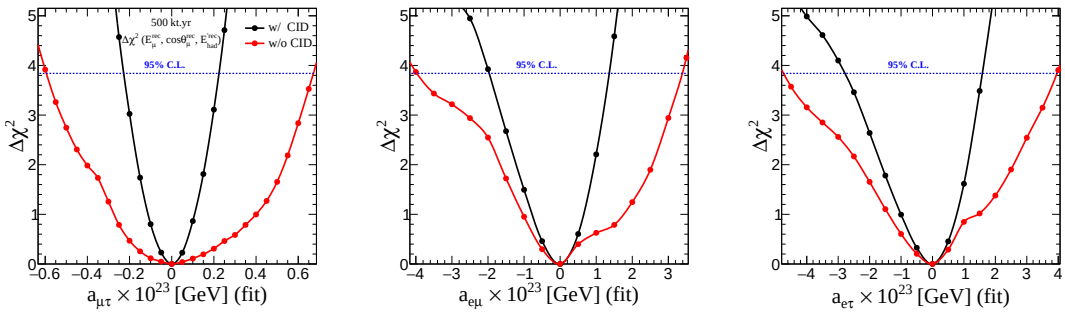

Figure 3. The constraints on LIV parameters $a_{\mu\tau}$, $a_{e\mu}$, and $a_{e\tau}$ at 95% C.L (1d.o.f) using 500 kt·yr exposure of the ICAL detector. The black curves represent $\Delta\chi^2$ with CID and the red curves represent $\Delta\chi^2$ without CID. These figures have been taken from Ref. [4].

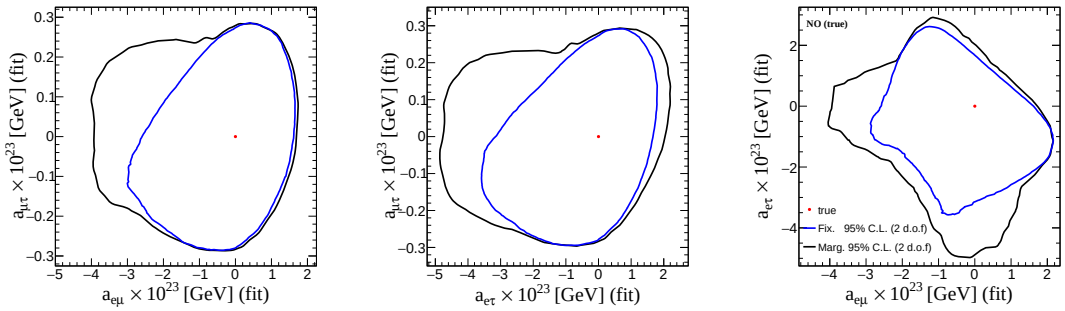

Figure 4. The constraints on correlated $a_{\mu\tau}$, $a_{e\mu}$, and $a_{e\tau}$ considered two-at-a-time at 95% C.L (2d.o.f) using 500 kt·yr exposure of the ICAL detector. These figures have been taken from Ref. [4].

Constraints on CPT-violating LIV parameters				
Experiments		$a_{\mu\tau}[10^{-23}$ GeV]	$a_{e\mu}[10^{-23}$ GeV]	$a_{e\tau}[10^{-23}$ GeV]
IceCube (99% C.L.)		$\lvert\mathrm{Re}(a_{\mu\tau})\rvert < 0.29$ $\lvert\mathrm{Im}(a_{\mu\tau})\rvert < 0.29$	–	–
Super-K (95% C.L.)		$\mathrm{Re}(a_{\mu\tau}) < 0.65$ $\mathrm{Im}(a_{\mu\tau}) < 0.51$	$\mathrm{Re}(a_{e\mu}) < 1.8$ $\mathrm{Im}(a_{e\mu}) < 1.8$	$\mathrm{Re}(a_{e\tau}) < 4.1$ $\mathrm{Im}(a_{e\tau}) < 2.8$
ICAL (95% C.L.)	w/o CID	$-0.59 \leq \mathrm{Re}(a_{\mu\tau}) \leq 0.67$	$-3.97 \leq \mathrm{Re}(a_{\mu\tau}) \leq 3.37$	$-4.71 \leq \mathrm{Re}(a_{\mu\tau}) \leq 3.96$
	w/ CID	$-0.23 \leq \mathrm{Re}(a_{\mu\tau}) \leq 0.22$	$-1.97 \leq \mathrm{Re}(a_{\mu\tau}) \leq 1.34$	$-2.80 \leq \mathrm{Re}(a_{\mu\tau}) \leq 1.58$

Table 2. A comparison of existing bounds on $a_{\mu\tau}$, $a_{e\mu}$, and $a_{e\tau}$ set by IceCube and Super-K with the bounds obtained by the ICAL detector. This Table has been taken from Ref. [4].

In Fig. 4, we estimate the $\Delta\chi^2$ sensitivity to constrain the correlated $(a_{e\mu}, a_{\mu\tau})$, $(a_{e\tau}, a_{\mu\tau})$ and $(a_{e\mu}, a_{e\tau})$ two-at-a-time with 95% C.L. Here, the black curves correspond to the contours which limit the CPT-violating parameters with marginalization over the oscillation parameters mentioned above, whereas the blue curves correspond to the fixed parameters scenario. In Table. 2, we compare the bounds obtained in this work [4] with the existing limits set by Super-K [7] and IceCube [8] experiments.

4. Summary

The upcoming magnetised ICAL detector at INO can play a crucial role to establish three-flavor neutrino oscillations in the multi-GeV energy range over a wide range of baselines by observing atmospheric neutrinos (ν_μ) and antineutrinos ($\bar{\nu}_\mu$) separately. The primary goals of ICAL are to determine mass ordering (MO) and precise measurement of neutrino oscillation parameters at the 2-3 sector. Using its excellent muon detection sensitivity, we explore CPT-violating LIV parameters $a_{\mu\tau}$, $a_{e\mu}$, and $a_{e\tau}$ in detail with an exposure of 500 kt·yr and place a stringent limit on these parameters.

References

[1] Colladay D and Kostelecky V A 1997 *Phys. Rev. D* **55** 6760–6774 (*Preprint* `hep-ph/9703464`)
[2] Ahmed S *et al.* (ICAL) 2017 *Pramana* **88** 79 (*Preprint* `1505.07380`)
[3] Kostelecky V A and Mewes M 2004 *Phys. Rev. D* **69** 016005 (*Preprint* `hep-ph/0309025`)
[4] Sahoo S, Kumar A and Agarwalla S K 2021 (*Preprint* `2110.13207`)
[5] Nunokawa H, Parke S J and Zukanovich Funchal R 2005 *Phys. Rev. D* **72** 013009 (*Preprint* `hep-ph/0503283`)
[6] Esteban I, Gonzalez-Garcia M C, Maltoni M, Schwetz T and Zhou A 2020 *JHEP* **09** 178 (*Preprint* `2007.14792`)
[7] Abe K *et al.* (Super-Kamiokande) 2015 *Phys. Rev. D* **91** 052003 (*Preprint* `1410.4267`)
[8] Aartsen M G *et al.* (IceCube) 2018 *Nature Phys.* **14** 961–966 (*Preprint* `1709.03434`)